

# Probing chromatic onsets of gravitational wave overtones

Hai-Tian Wang,<sup>1,2</sup> Yi-Ming Hu,<sup>3</sup> and Yi-Zhong Fan<sup>1,2,\*</sup>

<sup>1</sup>*Key Laboratory of Dark Matter and Space Astronomy, Purple Mountain Observatory, Chinese Academy of Sciences, Nanjing 210023, People's Republic of China*

<sup>2</sup>*School of Astronomy and Space Science, University of Science and Technology of China, Hefei, Anhui 230026, People's Republic of China*

<sup>3</sup>*TianQin Research Center for Gravitational Physics and School of Physics and Astronomy, Sun Yat-sen University (Zhuhai Campus), Zhuhai 519082, People's Republic of China*

(Dated: March 14, 2022)

The ringdown data of both GW150914 and GW190521.074359 (GW190521r) show evidence supporting the presence of overtone. Previous studies all adopt a fundamental assumptions, which were motivated more by convenience than by first principles, that the first overtone and the fundamental mode share a same onset. In this work, for the first time we relax such assumption, and we aim to probe the possible chromatic onsets of these two components within the GW150914 and GW190521r ringdown data. For both events, we bound the onset lags to be  $\Delta t_0 \leq 10M_f$  at high probabilities (i.e.,  $\geq 96.5\%$ ), where  $M_f$  is the mass of the remnant black hole formed in the merger. Moreover, for GW190521r (GW150914) we have  $\Delta t_0 \geq 3M_f$  at 98.3% (69.5%) credibility, indicating the non-simultaneous excitation between the fundamental mode and the first overtone in the ringdown.

## I. INTRODUCTION

A single distorted black hole will be formed after the violent plunge of compact binary black holes (BBHs). The gravitational wave (GW) radiation in this stage is called ringdown, after which it settles to a stationary state. The ringdown stage is described by the superposition of quasinormal modes (QNMs), in the form of damped sinusoids [1–3]. Recently, Isi *et al.* [4] find evidence of the existence of overtone mode in the ringdown signal of GW150914 [5]. Furthermore, Giesler *et al.* [6] confirm the importance of the overtone modes by analyzing ringdown signal from numerical relativity (NR) simulation. Later on, Abbott *et al.* [7] reveal the existence of overtone mode in GW190521.074359 (GW190521r).

Normally, analyses on ringdown data are performed in the time domain (TD) due to the abrupt start. Compared with the frequency domain analysis, TD analysis does not suffer from the Fourier frequency mixing problem [4, 8]. It has been developed to extract the properties of the remnant BH with GW data [6, 8, 9]. TD analysis based on ringdown data has also been used to test general relativity [10], no-hair theorems [4, 11, 12], and the BH area law [13]. A detailed introduction to different TD methods can be found in Isi and Farr [14].

The start time of the ringdown signal is an important and attractive problem, which is not finally solved yet. The numerical relativity (NR) simulations suggest that the start time of the fundamental mode is  $10 - 16M_f$  after the peak amplitude [15, 16], where  $M_f$  is the remnant mass. The analyses of the real GW data [4, 8, 9] are in favor of the presence of such a time delay. However, such conclusion might not be applicable to the overtone modes, for which it is found out that the ringdown signal starts from the peak strain amplitude [4, 6]. One

assumption made in such analyses is that the first overtone and the fundamental mode were excited simultaneously [4, 6]. We remark that such assumption was motivated mainly for convenience of calculation, instead of first-principles[17]. Therefore, it is meaningful to examine such assumption in detail with real data.

In this work, we re-analyze the ringdown data of GW150914 and GW190521r, allowing different start times for the first overtone and the fundamental mode. For both events, the onset lags between the first overtone and the fundamental mode are bounded to be within a time of  $10M_f$  at high probabilities (i.e.,  $\geq 96.5\%$ ). Moreover, for GW190521r the onset lag is found to be larger than  $3M_f$  at 98.3% credibility. The method we adopted is introduced in Sec. II, and the main results will be presented in Sec. III. Finally, we summarize this work in Sec. IV. We assume  $G = c = 1$  throughout the paper, unless otherwise specified.

## II. METHOD

In general relativity, the ringdown waveform of Kerr BH is fully described by two time-dependent polarization  $h(t) = h_+(t) - ih_\times(t)$ , which can be written as

$$h_+(t) - ih_\times(t) = \sum_l \sum_m \sum_n^N A_{lmn} \exp(i(-\Omega_{lmn}(t - \Delta t_n) + \phi_{lmn})) \times {}_{-2}Y_m(\iota), \quad (1)$$

where  $N$  is the total overtone numbers,  $A_{lmn}$  ( $\phi_{lmn}$ ) characterize the amplitudes (phases) of each ringdown mode at the peak,  $\Delta t_n$  represents the time delay of mode  $n$ ,  $\iota$  is the inclination angle, and  ${}_{-2}Y_m(\iota)$  are the spin-weighted spherical harmonics [6]. The response of a sin-

\* yzfan@pmo.ac.cn

gle detector  $k$  to the gravitational waves is described as

$$h_k(t) = F_k^+(\theta, \phi, \psi)h_+(t) + F_k^\times(\theta, \phi, \psi)h_\times(t), \quad (2)$$

where  $F_k^{+, \times}(\theta, \phi, \psi)$  are the antenna beam patterns,  $\theta, \phi$  are the longitudinal and azimuthal angles, and  $\psi$  is the polarization angle.

The gravitational wave data stream  $d$  is provided by the Gravitational-Wave Open Science Center [18], which contains the signal  $h(t)$  and noise  $g(t)$ . In standard gravitational wave data analysis, the detector noise can be assumed to be a Gaussian stochastic process [19]. As a Gaussian stochastic process, each set  $[g(t_0), g(t_1), \dots, g(t_{G_s-1})]$  is distributed as multivariate Gaussian probability density function (PDF),

$$\mathbf{g}(\mathbf{t}) \sim \mathcal{G}(\boldsymbol{\mu}, \boldsymbol{\Sigma}), \quad (3)$$

where  $\boldsymbol{\mu}$  and  $\boldsymbol{\Sigma}_{ij} = \rho(i-j)$  are the mean and the covariance matrix of the noise time series, respectively. After applying a high-pass filter with a roll-on frequency of 20 Hz, the data stream can be treated as zero mean. Then we assume that the noise in the detector is stationary.  $\rho$  is the auto-covariance function

$$\rho(i-j) = \langle g_i g_j \rangle, \quad (4)$$

and  $\rho(-n) = \rho(G_s - g)$  for  $0 \leq g < G_s$ , where  $G_s$  is the total number of samples.

On the one hand, one can get the covariance matrix by calculating the auto-covariance function (ACF) from GW data directly. On the other hand, according to the Wiener-Khinchin theorem, the auto-covariance function is the inverse Fourier transform of the power spectral density (PSD). Thus, one can also get the covariance matrix by calculating the PSD from the GW data, then truncate it with proper duration to break circularity. We apply these two solutions to GW150194 and GW190521r respectively.

For gravitational wave data analysis in time domain, the inner product between two waveforms  $h_1(t)$  and  $h_2(t)$  can be defined as

$$(h_1 | h_2) = h_1^T \boldsymbol{\Sigma}^{-1} h_2. \quad (5)$$

Given the observed strain series  $d_k(t)$  and the gravitational wave signal  $h_k(t)$  from waveform model, the log-likelihood function can be written as

$$\log \mathcal{L}_k = -\frac{1}{2}(d_k - h_k | d_k - h_k). \quad (6)$$

The log-likelihood function of multiple detectors is the sum of the individual log-likelihood.

We carry out Bayesian inference with BILBY package [20] and PYMULTINEST sampler [21] with 5000 live points. For the TD ringdown analyses, Bayesian inferences are performed with 0.5 seconds data stream that start from the peak strain amplitude. The priors on the final mass  $M_f$  are  $[50, 100]M_\odot$  and  $[50, 120]M_\odot$  for

GW150914 and GW190521r, respectively. Following Isi *et al.* [4] and Abbott *et al.* [9], we fix some extrinsic parameters for GW150914 (GW190521r): the geocentric time is set to be 1126259462.408665(1242459857.472) GPS, the right ascension is  $\alpha = 1.95(5.46)$  rad, the declination is  $\delta = -1.27(0.59)$  rad, the polarization angle is  $\psi = 0.82(1.37)$  rad, and the inclination angle is  $\iota = \pi(2.64)$  rad. For other parameters, they are the same for both GW150914 and GW190521r. The priors on the dimensionless spin  $\chi_f$ , the amplitudes parameter  $A_{lmn}$ , and the phase parameter  $\phi_{lmn}$  are uniformly distributed in the ranges of  $[0, 0.99]$ ,  $[0, 25]$ , and  $[0, 2\pi]$ , respectively.

### III. RESULTS

There are 50 GW events reported by Advanced LIGO and Advanced Virgo during the first two Gravitational-Wave Transient Catalogs [7, 18]. Among them, GW150914 and GW190521r have the strongest ringdown signals and show tentative evidence for the first overtone [9]. For other events, the ringdown signals are weak and no evidence for higher modes is found and they can hardly be adopted in this work since the fundamental mode tends to match the peak of the strain if one does not fix the start time. Thus, our analyses focus on GW150914 and GW190521r. We assume that the first overtone starts from the peak and then varies the start time of the fundamental mode. Equivalently, we set  $\Delta t_1 = 0$  and assume a uniform prior on  $\Delta t_0$  in the range of  $[0, 20] M_f$ .

In FIG. 1, we summarize the main results of our analysis. Interestingly, the distribution of  $\Delta t_0$  of GW150914 shows a bimodal structure. The major part of the bimodal distribution ranges from  $3 M_f$  to  $12 M_f$  (with 69.5% probability) and the minor part is approaching  $0 M_f$  (with 30.5% probability). The major part represents the deviation between the start times of the overtone mode and the fundamental mode. A  $\Delta t_0 \geq 10 M_f$  has been rejected at 96.5% credible level.

For GW190521r, encouragingly, the distribution of  $\Delta t_0$  is strongly in favor of that there is a deviation between the start times of the overtone mode and the fundamental mode. The probability for  $\Delta_0 \geq 3 M_f$  is 98.3%. Similar to GW150914, a bound on  $\Delta t_0 \leq 10 M_f$  is favored at a high credible level (99.5%).

Additionally, we also perform TD Bayesian inferences on GW150914 and GW190521r with  $\Delta t_0 = 0$ , as comparison. We show the posterior distributions of the redshifted final masses and spins for GW150914 and GW190521r in FIG. 2. In the case of  $\Delta t_0 = 0$ , our results are in agreement with those of Abbott *et al.* [9], as anticipated. Compared with the case of  $\Delta t_0 = 0$ , the distributions of the parameters for  $\Delta t_0 \neq 0$  of both events are broader. This is reasonable since an additional parameter ( $\Delta t_0$ ) has been introduced into the ringdown waveform modeling.

In TABLE. I, we show the corresponding 90%-credible

## IV. CONCLUSIONS

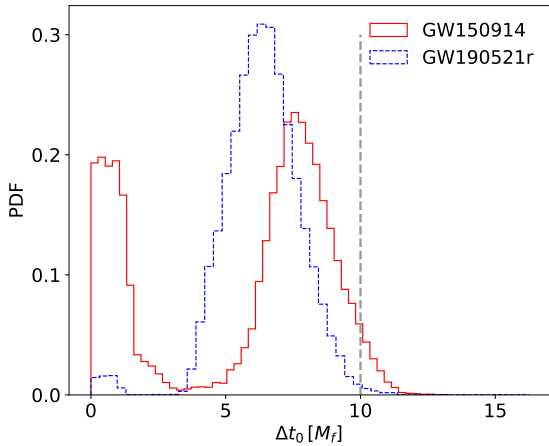


FIG. 1: Distributions of  $\Delta t_0$  of GW150914 (red histogram) and GW190521r (dashed blue histogram). We measure  $\Delta t_0 = 7.11_{-6.85}^{+2.67}$  ( $7.11_{-6.85}^{+2.67}$ ) at 90% credibility for GW150914 (GW190521r). The dashed gray line marks the time  $10 M_f$  later than the peak of the ringdown signal. For GW150914 (GW190521r), the probability that  $\Delta t_0 < 10 M_f$  is 96.5% (99.5%) and the probability that  $\Delta t_0 > 3 M_f$  is 69.5% (98.3%).

TABLE I: The median and symmetric 90%-credible intervals, of the redshifted final mass, final spin, and  $\Delta t_0$ , inferred from the ringdown analyses of GW150914 and GW190521r. We quantify the choice of different priors on  $\Delta t_0$  using log Bayes factor  $\log_{10} \mathcal{B}_{\Delta t_0 \neq 0}^{\Delta t_0 = 0}$ . The first overtone has been taken into account in the ringdown analyses.

Events	$M_f [M_\odot]$	$\chi_f$	$\Delta t_0$	$\log_{10} \mathcal{B}_{\Delta t_0 = 0}^{\Delta t_0 \neq 0}$
GW150914	$69.7_{-11.7}^{+12.0}$	$0.63_{-0.41}^{+0.20}$	0	-
	$70.4_{-13.9}^{+14.6}$	$0.66_{-0.45}^{+0.20}$	$7.11_{-6.85}^{+2.67}$	-0.4
GW190521r	$91.6_{-14.3}^{+14.3}$	$0.77_{-0.24}^{+0.12}$	0	-
	$86.4_{-20.1}^{+20.0}$	$0.69_{-0.49}^{+0.19}$	$6.37_{-2.09}^{+2.23}$	+0.6

measurements of  $M_f$ ,  $\chi_f$ , and  $\Delta t_0$ . To quantify the contribution of  $\Delta t_0$ , we calculate the log Bayes factor versus the fixed case. For GW150914 (GW190521r), the log Bayes factor of  $\Delta t_0 \neq 0$  is  $\log_{10} \mathcal{B}_{\Delta t_0 = 0}^{\Delta t_0 \neq 0} = -0.4 (+0.6)$ . There may indicate the presence of  $\Delta t_0$  for GW190521r, but unclear for GW150914. This may be due to the bimodal distribution of  $\Delta t_0$  for GW150914, as shown in FIG. 1. Thus, for this event we also perform analyses by assuming different uniform priors on  $\Delta t_0$ , which are  $0 M_f < \Delta t_0 < 3 M_f$  and  $3 M_f < \Delta t_0 < 20 M_f$ , respectively. The  $\log_{10}$  Bayes factor of the former versus the later is just +0.1.

In this work, we analyze the ringdown signal of GW150914 and GW190521r with the first overtone and the fundamental mode, allowing different start times of these two components. The traditional treatment that assumes a same onset time for different modes are simpler, but lack physical motivation; the different onset time assumption, on the other hand, are more physical but also more complex. The Bayes factor, which penalises complicated models quantitatively, does not show decisive conclusions on either model. This indicates that more and better-quality observations are required to give definitive answer to the simultaneousness of different modes onset. However, if we abandon the same onset assumption, then the data show support to a clear difference. For both GW150914 and GW190521r, there are tentative indication for the delayed onset of the fundamental mode in comparison to the first overtone. For GW150914, the resulting distribution of  $\Delta t_0$  has a distinct bimodal structure, and we have  $\Delta t_0 \geq 3 M_f$  at the credible level of 69.5%. For GW190521r, the “evidence” is stronger and we have  $\Delta t_0 \geq 3 M_f$  at 98.3% credible level. A very robust upper bound can be set as  $\Delta t_0 \leq 15 M_f$ . In reality, we have  $\Delta t_0 \leq 10 M_f$  at the confidence levels of 96.5% and 99.5% for GW150914 and GW190521r, respectively. These results are interesting since the NR simulation results suggest that the fundamental mode should start from  $10 - 16 M_f$  later than the peak strain amplitude [15, 16] and it was also speculated that the overtones were not excited simultaneously [17]. Note that the first overtone is assumed to start from the peak strain amplitude in our analysis, which may lead to an earlier onset time of the fundamental mode. We aim to relax such assumptions whence better-quality data is available.

In summary, by abandoning the simultaneous onset assumption for different modes, the ringdown data of GW150914 and GW190521r indicate a clear chromatic onsets of the first overtone and the fundamental mode. Moreover, we measure the separation between the start times of the first overtone and the fundamental mode to be within  $10 M_f$  at 96.5% (about  $2\sigma$ ) credibility. We stress that the current data can not draw a decisive conclusion and more accumulation of data is needed to better resolve this issue.

## ACKNOWLEDGMENTS

We sincerely thank Maximiliano Isi, Peng-Cheng Li, and Shao-Peng Tang for the relevant discussions. This work has been supported by NSFC under Grants No. 11921003, No. 11847241, No. 12173104, and No. 12047550. H.T.W. is also supported by the Opening Foundation of TianQin Research Center. This research has made use of data, software, and/or web tools obtained from the Gravitational Wave Open Science Cen-

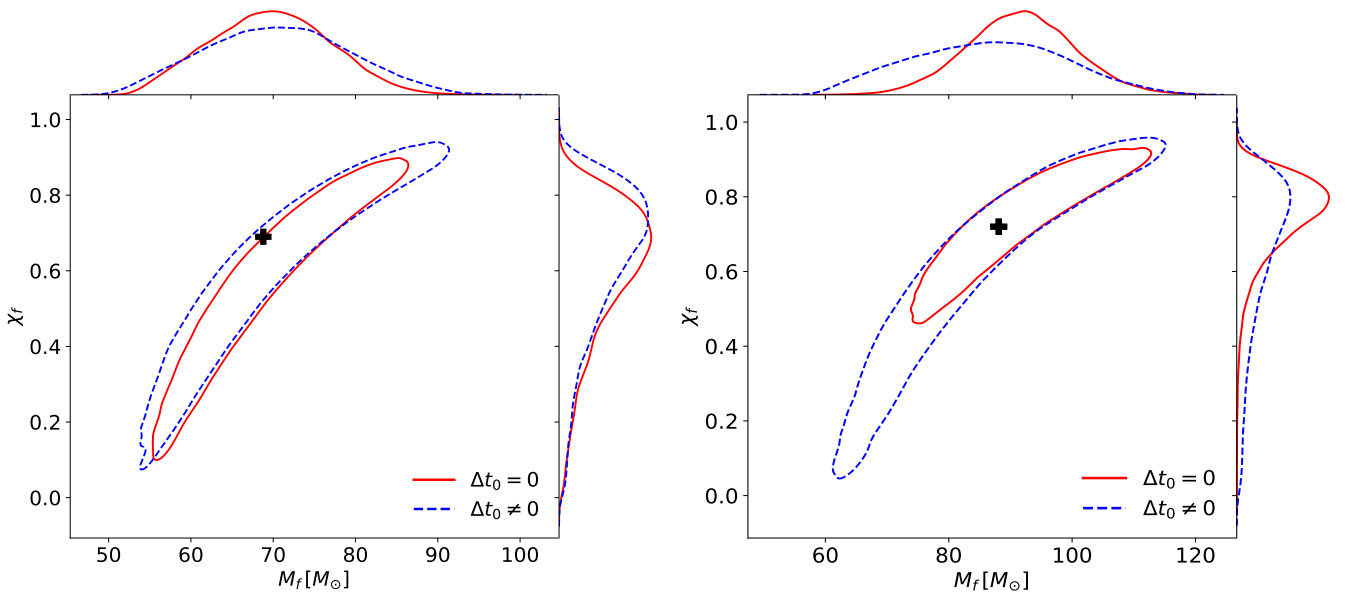


FIG. 2: Posterior distributions of the redshifted final mass and final spin for GW150914 (left panel) and GW190521r (right panel). The red (dashed blue) contour represents the result assuming there is a deviation (no deviation) between the overtone mode and the fundamental mode. All of these contours are 90%-credible regions. The 1D marginalized posterior distributions for the final mass and the final spin are shown in the top and right-hand panels, respectively. For GW150914 (GW190521r), the median values of the final mass  $M_f = 68.8 M_\odot$  ( $88.1 M_\odot$ ) and final spin  $\chi_f = 0.69$  ( $0.72$ ) given by the full IMR analysis [9], which is shown as a black plus marker.

ter (<https://www.gw-openscience.org>), a service of LIGO Laboratory, the LIGO Scientific Collaboration, and the Virgo Collaboration. LIGO is funded by the U.S. National Science Foundation. Virgo is funded by the French

Centre National de Recherche Scientifique (CNRS), the Italian Istituto Nazionale della Fisica Nucleare (INFN), and the Dutch Nikhef, with contributions by Polish and Hungarian institutes.

- 
- [1] C. V. Vishveshwara, *Phys. Rev. D* **1**, 2870 (1970).  
[2] W. H. Press, *Astrophysical Journal, Letters* **170**, L105 (1971).  
[3] S. A. Teukolsky, *Astrophysical Journal* **185**, 635 (1973).  
[4] M. Isi, M. Giesler, W. M. Farr, M. A. Scheel, and S. A. Teukolsky, *Phys. Rev. Lett.* **123**, 111102 (2019).  
[5] R. Abbott, T. D. Abbott, S. Abraham, F. Acernese, K. Ackley, A. Adams, C. Adams, R. X. Adhikari, V. B. Adya, C. Affeldt, and et al., *Phys. Rev. Lett* **116**, 061102 (2016), [arXiv:1602.03837 \[gr-qc\]](https://arxiv.org/abs/1602.03837).  
[6] M. Giesler, M. Isi, M. A. Scheel, and S. A. Teukolsky, *Physical Review X* **9**, 041060 (2019), [arXiv:1903.08284 \[gr-qc\]](https://arxiv.org/abs/1903.08284).  
[7] R. Abbott, T. D. Abbott, S. Abraham, F. Acernese, K. Ackley, A. Adams, C. Adams, R. X. Adhikari, V. B. Adya, C. Affeldt, and et al., *Physical Review X* **11**, 021053 (2021), [arXiv:2010.14527 \[gr-qc\]](https://arxiv.org/abs/2010.14527).  
[8] G. Carullo, W. Del Pozzo, and J. Veitch, *Phys. Rev. D* **99**, 123029 (2019).  
[9] R. Abbott *et al.* (LIGO Scientific, Virgo), *Phys. Rev. D* **103**, 122002 (2021), [arXiv:2010.14529 \[gr-qc\]](https://arxiv.org/abs/2010.14529).  
[10] H.-T. Wang, S.-P. Tang, P.-C. Li, and Y.-Z. Fan, *arXiv e-prints*, [arXiv:2104.07594](https://arxiv.org/abs/2104.07594) (2021), [arXiv:2104.07594 \[gr-qc\]](https://arxiv.org/abs/2104.07594).  
[11] S. W. Hawking, *Commun. Math. Phys.* **25**, 152 (1972).  
[12] D. C. Robinson, *Phys. Rev. Lett.* **34**, 905 (1975).  
[13] M. Isi, W. M. Farr, M. Giesler, M. A. Scheel, and S. A. Teukolsky, *Phys. Rev. Lett* **127**, 011103 (2021), [arXiv:2012.04486 \[gr-qc\]](https://arxiv.org/abs/2012.04486).  
[14] M. Isi and W. M. Farr, *arXiv e-prints*, [arXiv:2107.05609](https://arxiv.org/abs/2107.05609) (2021), [arXiv:2107.05609 \[gr-qc\]](https://arxiv.org/abs/2107.05609).  
[15] L. London, D. Shoemaker, and J. Healy, *Phys. Rev. D* **90**, 124032 (2014), [arXiv:1404.3197 \[gr-qc\]](https://arxiv.org/abs/1404.3197).  
[16] S. Bhagwat, M. Okounkova, S. W. Ballmer, D. A. Brown, M. Giesler, M. A. Scheel, and S. A. Teukolsky, *Phys. Rev. D* **97**, 104065 (2018), [arXiv:1711.00926 \[gr-qc\]](https://arxiv.org/abs/1711.00926).  
[17] S. Bhagwat, X. J. Forteza, P. Pani, and V. Ferrari, *Phys. Rev. D* **101**, 044033 (2020), [arXiv:1910.08708 \[gr-qc\]](https://arxiv.org/abs/1910.08708).  
[18] B. P. Abbott *et al.* (LIGO Scientific Collaboration and Virgo Collaboration), *Phys. Rev. X* **9**, 031040 (2019).  
[19] B. P. Abbott *et al.* (LIGO Scientific Collaboration and Virgo Collaboration), *Phys. Rev. Lett.* **116**, 061102 (2016).  
[20] G. Ashton, M. Hübner, P. D. Lasky, C. Talbot, K. Ackley, S. Biscoveanu, Q. Chu, A. Divakarla, P. J. Easter, B. Goncharov, F. H. Vivanco, J. Harms, M. E. Lower,

G. D. Meadors, D. Melchor, E. Payne, M. D. Pitkin, J. Powell, N. Sarin, R. J. E. Smith, and E. Thrane, [The Astrophysical Journal Supplement Series](#) **241**, 27 (2019).  
[21] J. Buchner, A. Georgakakis, K. Nandra, L. Hsu,

C. Rangel, M. Brightman, A. Merloni, M. Salvato, J. Donley, and D. Kocevski, [A&A](#) **564**, A125 (2014), [arXiv:1402.0004 \[astro-ph.HE\]](#).